# The Characteristics of Carbon Nanotube-Reinforced Poly(phenylene sulfide) Nanocomposites

**Suzhu Yu,[1] Wai Mun Wong,[2] Xiao Hu,[2] Yang Kay Juay[1]**

[1]*Singapore Institute of Manufacturing Technology, 638075 Singapore*
[2]*School of Materials Engineering, Nanyang Technological University, 639798 Singapore*

Received 3 October 2007; accepted 26 January 2009
DOI 10.1002/app.30191
Published online 8 May 2009 in Wiley InterScience (www.interscience.wiley.com).

**ABSTRACT:** Multiwall carbon nanotube reinforced poly (phenylene sulfide) (PPS) nanocomposites were successfully fabricated through melt compounding. Structural, electrical, thermal, rheological, and mechanical properties of the nanocomposites were systematically studied as a function of carbon nanotube (CNT) fraction. Electrical conductivity of the polymer was dramatically enhanced at low loading level of the nanotubes; the electrical percolation threshold lay between 1 and 2 wt % of the CNTs. Rheological properties of the PPS nanocomposites also showed a sudden change with the CNT fraction; the percolation threshold was in the range of 0–0.5 wt % of CNTs. The difference in electrical and rheological percolation threshold was mainly due to the different requirements needed in the carbon nanotube network in different stages. The crystallization and melting behavior of CNT-filled PPS nanocomposites were studied with differential scanning calorimetry; no new crystalline form of PPS was observed in the nanocomposites, but the crystallization rate was reduced. The thermal and mechanical properties of the nanocomposites were also investigated, and both of them showed significant increase with CNT fraction. For 5 wt % of CNT-filled PPS composite, the onset of degradation temperature increased by about 13.5°C, the modulus increased by about 33%, and tensile strength increased by about 172%. © 2009 Wiley Periodicals, Inc. J Appl Polym Sci 113: 3477–3483, 2009

**Key words:** carbon nanotubes; nanocomposites; poly (phenylene sulfide); conducting polymers

## INTRODUCTION

Polymer composites with improved electrical properties have been widely used in various industries including electronics, biomedical devices, automotive, and aerospace as anti-static, electromagnetic shielding, and electrically conductive materials.[1,2] The conventional method to enhance electrical conductivity of polymers is to compound polymers with conductive fillers such as metal particles or carbon black; high loading of conductive fillers is usually needed to obtain the materials with high conductivity. This, however, not only increases the weight and final cost of the products but also often impairs the mechanical properties of the polymers. Thus, it is necessary to development polymer composites with both good electrical and mechanical properties.

Carbon nanotubes (CNTs), a new type of carbon filler, are thought to be ideal reinforcements for polymers due to their high aspect ratio and exceptionally superior mechanical, thermal, and electrical properties.[3,4] CNT-reinforced polymer nanocomposites possess the potential to be next generation of electrically conductive materials; they might have many advantages over conventional composites such as high electrical conductivity at very low CNT fraction; good thermal and mechanical performance with light weight and low viscosity allow them to be molded easily.

The commonly used methods to fabricate polymer nanocomposites with carbon nanotubes are *in situ* polymerization,[5–7] solution route,[8–11] and melt compounding.[12–14] For *in situ* polymerization, carbon nanotubes are mixed with monomers; a polymerization then starts either thermally or chemically. The solution route may consist of several steps: (a) dissolving matrix polymer into an appropriate solvent to make a solution; (b) dispersing carbon nanotubes into the solution to make a suspension; (c) casting the new mixture to evaporate the solvent to produce final nanocomposites. In the melt compounding process, carbon nanotubes are mixed with thermoplastic polymers at their molten state. The formation of nanocomposites depends on the thermodynamic interaction between the polymer chains and carbon nanotubes. Comparing these three approaches, melt compounding is a simple and versatile method to synthesize nanocomposites. The resultant nanocomposites have high purity as the process is essentially free of contaminations.

*Correspondence to:* S. Yu (szyu@simtech.a-star.edu.sg).

Poly(phenylene sulfide) (PPS) is an engineering polymer having a symmetrical, rigid backbone chain consisting of recurring para-substituted rings and sulfur atoms. It has good endurance at high temperatures and possesses excellent resistance to different aggressive chemicals.[15,16] The carbon nanotubes filled with PPS materials are expected to have appreciable improvements in thermal and mechanical properties and can find their applications as automotive engine compartment components, in fuel line systems, and other places where solvent resistance and/or exposure to high temperature is necessary.

In this study, the CNT-filled PPS nanocomposites are fabricated with melt compounding. The CNT concentration and fabrication parameters are optimized to obtain the nanocomposites with good thermal, electrical, and mechanical properties. The percolation of carbon nanotubes is described by measurements of the electrical resistivity and is compared with the results derived from the rheological evaluations.

## EXPERIMENTAL

Commercially available PPS (Chevron Philips Chemicals, Asia Pte Ltd, Singapore) and multiwall carbon nanotubes (Chinese Nanofiller Company, Beijing, P. R. of China) were used as matrix and filler, respectively. The MFI of the PPS is 185 g/10 min. The CNTs with purity of 92% are generated by chemical vapor deposition. They have an outer diameter of about 20 nm with a length of a few tens of micrometers.

PPS as well as the carbon nanotubes were predried at a temperature of 100°C overnight in an oven to remove any moisture before processing. Following that, the polymer and CNTs were mixed according to the weight ratios. The nanocomposites were fabricated with internal mixer of Haake Rheocord 90, which have counter-rotating screws. The processing temperature was maintained at 285°C and the rotor speed was set at 75 rpm. The palletized nanocomposites were then dried at a temperature of 100°C overnight. The samples for electrical testing were hot-pressed at 290° with uniaxial force of 50 kN. The samples for mechanical testing were injection-molded using a Battenfeld BA500 CDK-SE molding machine. The temperatures for injection molding were 295, 290, 280, and 280°C, respectively, for different zones. The dimension of the dumbbell-shaped samples was about 80 mm in length, 5 mm in width, and 2 mm in thickness.

The morphology of the carbon nanotubes and fracture surfaces of the nanocomposites were observed with a field emission scanning electron microscope (FESEM, Jeol JSM 6340F). The dispersion and orientation of CNTs in the nanocomposites were observed by transmission electron microscopy (TEM, Philips CM300). For TEM sample preparation, ultrathin sections of the nanocomposites with a thickness of $\sim$ 70 nm were cut accordingly using an ultramicrotome (Leica Ultracut UCT) equipped with water flotation and a diamond knife.

The volume electrical resistivity of the nanocomposites was determined by two probes method. The resistance of the samples was measured using High Resistance Meters (Hewlett Packard 4339B) if the resistance was very high or using multimeter (Fluke 85) if the resistance was low. The resistivity of the nanocomposites was then calculated by following equation:

$$\rho = \frac{RA}{t} \tag{1}$$

where $\rho$ is the volume resistivity ($\Omega$ m), $R$ is the volume resistance ($\Omega$), $A$ is the area of the sample contacting the electrode ($m^2$), and $t$ is the thickness of the sample (m).

The thermal properties of the nanocomposites were investigated with TA 2920 differential scanning calorimeter (DSC) and TA Q500 thermal gravimetric analyzer (TGA). The heating rate was 5°C/min for DSC and 10°C/min for TGA. All experiments were run under a nitrogen purge. The degree of crystallinity (DOC) of samples was calculated using DSC data according the following equation[17]:

$$\mathrm{DOC} = \frac{\Delta H_m}{\Delta H_f (1 - W_f)} \times 100 \tag{2}$$

where $W_f$ is the weight fraction of the CNT filler in the nanocomposite, $\Delta H_m$ is the enthalpy of fusion, and $\Delta H_f$ is the enthalpy of fusion for a 100% crystalline PPS; it is taken as 50.16 J/g according to the literature.[18,19]

Rheological properties of the nanocomposites were measured using Kayeness capillary rheometer with die diameter of 1.0 mm. In the testing, about 10 g of the sample was loaded into chamber, which was heated to 285°C. The sample was then forced through a die at regulated shear rates. Viscosity was measured accordingly and plotted with respect to the shear rate.

The mechanical properties of the nanocomposites were measured with Instron 4505 tensile machine at room temperature. The crosshead speed used was 50 mm/min. At least five samples were tested for every nanocomposites; the final property were the average of the five measured results.

## RESULTS AND DISCUSSION

Figure 1 shows the FESEM micrograph of the multiwall carbon nanotubes. Many tubes can be seen loosely entangled together without obvious particle-

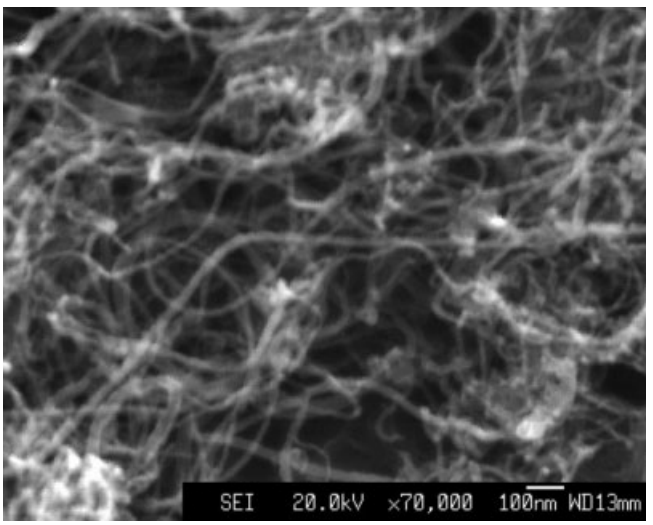


**Figure 1** FESEM micrograph of the multiwall carbon nanotubes.

like impurities. The diameter of the nanotubes is about 15–20 nm. Figure 2 shows the TEM image of 2 wt % carbon nanotube filled PPS nanocomposites. The tubes are arranged randomly and dispersed homogeneously in the polymer matrix. No apparent damage or breakdown of the nanotubes is observed.

PPS are excellent insulating material, with electrical resistivity of about $10^{16}$ Ω cm, whereas carbon nanotubes have electrical characteristics that are similar to metallic/semimetallic materials. The addition of the CNTs into the polymer improves its electrical conductivity. Figure 3 shows the resistivity of the PPS nanocomposites, measured at room temperature, as a function of CNT concentration. The electrical resistivity decreases monotonously with CNT fraction and exhibits a percolation. The percolation threshold, a critical concentration of filler where the resistivity starts to reduce abruptly, lies between 1 and 2 wt % of CNTs; the electrical resistivity of the samples changes over more than 11 orders of magnitude in this range. Further increasing the amount of CNTs beyond the percolation threshold, the electrical resistivity only decreases marginally. The percolation threshold of the CNT-filled polymer is very low as compared with spherical carbon particle-based polymers. This is a result of the high aspect ratio of CNT filler and homogeneous dispersion of the CNTs in the polymer matrix. Moreover, the conducting network formed by the CNTs is robust and less segregated, and the percolation curve of CNT filled polymer is not so steep; it is, thus, easier to precisely control the level of electrical resistance for the material. Several other groups have also reported an increase in the electrical conductivity for CNT-reinforced polymer composites.[20–22] Barraza et al.[23] reported a decrease in the electrical resistivity of a CNT-filled polystyrene composite from $10^{16}$ to $10^{6}$ Ω cm, with a threshold at about 6 wt % of CNT.

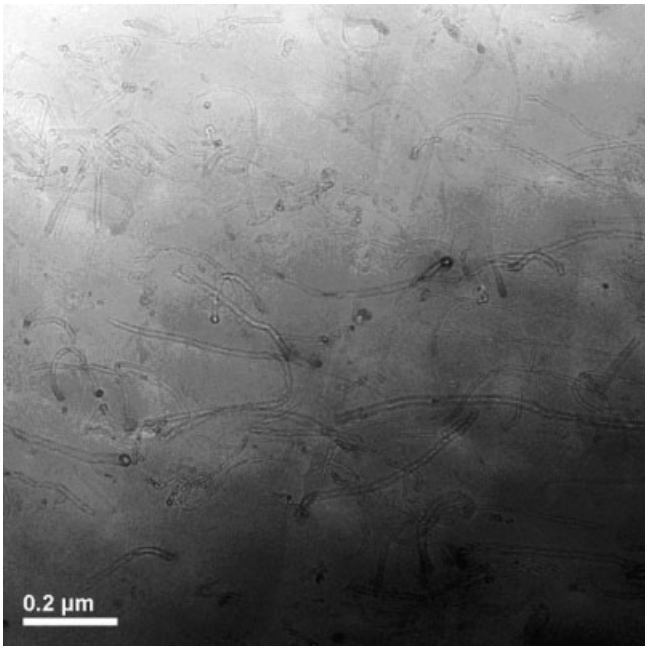


**Figure 2** TEM micrograph of the PPS nanocomposite with 2 wt % of CNTs.

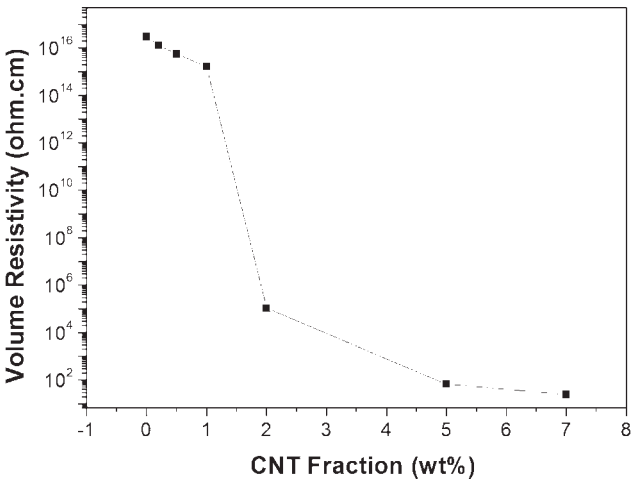


**Figure 3** Resistivity of the nanocomposites as a function of CNT fraction.

The dependency of the electrical resistivity of the PPS nanocomposites on temperature has also been investigated, as shown in Figure 4. The resistivity of both neat PPS and CNTs-filled composites is found to be almost temperature independent in the experimental range from 20 to 200°C, indicating that the materials are thermally stable in electrical property. Thus, when the nanocomposites are used in electronic devices, there is no compromise in their electrical properties when temperature changes.

Figure 5 shows the TGA profiles as a function of CNT fraction. The onset of decomposition of the nanocomposites occurs at higher temperatures than

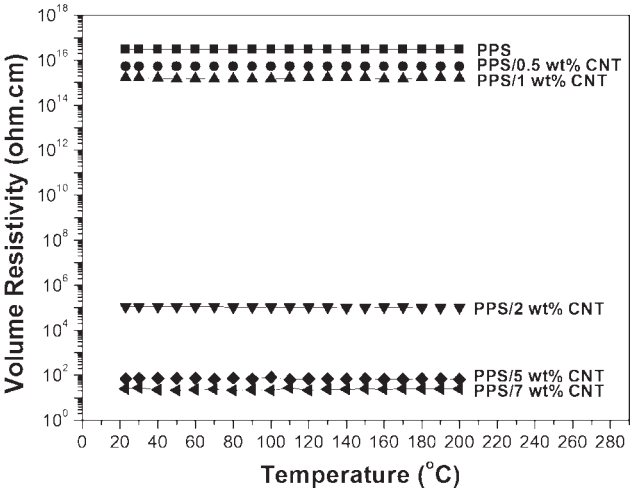


**Figure 4** Temperature dependency of the resistivity of the PPS nanocomposites.

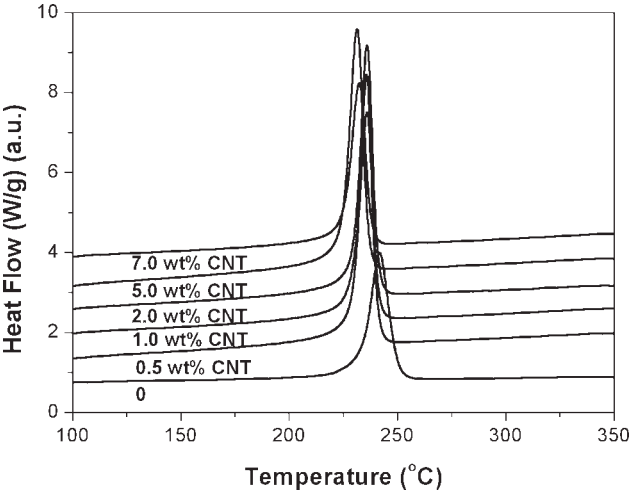


**Figure 6** DSC cooling curves of the PPS nanocomposites.

that of neat PPS. The increment is about 13.5°C for 5 wt % of CNT filled PPS nanocomposite from 476°C for neat PPS to 489.5°C of the nanocomposite. The incorporation of CNTs into the PPS offers a great stabilizing effect.

Information regarding the crystallization behavior of the nanocomposites can be obtained from DSC evaluation. Figures 6 and 7 show the second heating and cooling DSC curves of PPS with different amounts of carbon nanotubes. Both neat PPS and its nanocomposites have one exothermic and one endothermic peak, suggesting that the addition of CNTs does not result in a formation of new crystalline forms of PPS. However, the peak melting temperatures ($T_m$) and peak crystallization temperatures ($T_c$) shift to a lower end with increasing CNT content as tabulated in Table I. For the peak melting temperature of the nanocomposites, the variation is less than 2°C in the experimental range, but the crystalline temperature has stronger dependence on the CNT fraction. With the addition of 0.5 wt % of carbon nanotubes, the peak crystallization temperature is about 6.0°C lower compared with neat PPS. By further addition of CNTs, the decrease in $T_c$ is less significant; the $T_c$ is about 10.3°C lower than that of neat PPS for the CNT/PPS composite with 5 wt % CNT.

In addition to the melting and crystallization temperatures, the carbon nanotubes incorporated may also affect other crystallization behaviors of the polymer, such as degree of crystallinity and crystallization rate. The impact on the DOC is considered according to eq. (2); results are given in Table I. It can be seen that the DOC of the samples with different amounts of CNTs shows only small variations ranging between 79.90% and 77.51%. Regarding to crystallization rate, it is generally known that the degree of supercooling ($\Delta T$), which is defined by the difference between the peak melting temperature and onset crystallization temperature, can be used to

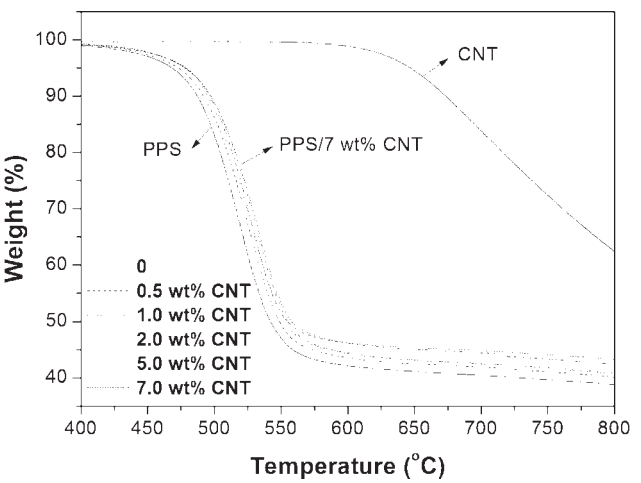


**Figure 5** TGA profile of the PPS nanocomposites.

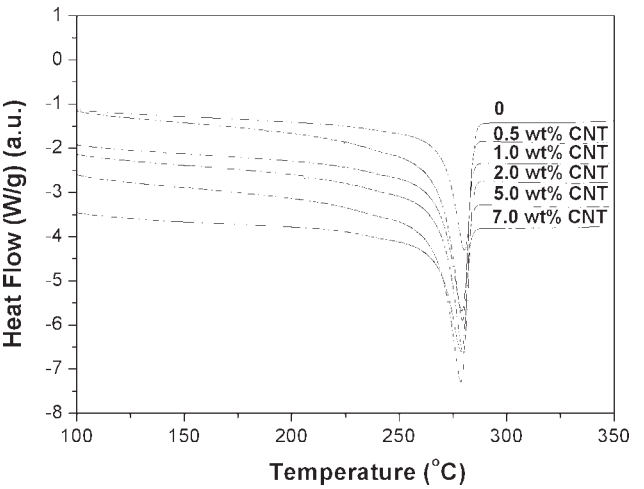


**Figure 7** DSC heating curves of the PPS nanocomposites.

**TABLE I**
**DSC Results of CNT-Filled PPS Nanocomposites**

| CNT fraction (wt %) | $T_m$ (°C) | $T_c$ (°C) | DOC (%) | $\Delta T$ |
|---|---|---|---|---|
| 0 | 280.36 | 241.75 | 79.90 | 29.31 |
| 0.5 | 279.39 | 235.79 | 78.02 | 37.54 |
| 1 | 279.17 | 235.94 | 78.86 | 36.93 |
| 2 | 279.76 | 235.93 | 79.72 | 36.26 |
| 5 | 278.69 | 231.37 | 77.51 | 40.35 |
| 7 | 278.75 | 232.40 | 78.07 | 40.17 |

characterize the crystallization rate of polymer melts. An increase in $\Delta T$ generally indicates that the crystallization rate of polymer is decreased.[24] The $\Delta T$ values for different CNTs-filled PPS are calculated and shown in Table I. In contrast to the degree of crystallinity, the crystallization rate is greatly affected by the addition of CNTs. The $\Delta T$ increases obviously from 29.31 to 37.54°C after incorporation of only 0.5 wt % of CNTs; that is, the crystallization rate is reduced by incorporating CNT filler. On further addition of CNTs, the increase in $\Delta T$ becomes smaller, and the $\Delta T$ for 5 wt % CNT reinforced nanocomposite is about 40.35°C. The decrease in crystallization rate indicates that the dispersion of CNT in the polymer matrix hinders the molecular movements in the melt state. It also explains why the crystallization temperature shifts to lower temperatures with CNT fraction.

Usually, addition of particles to polymer melts can cause processing difficulties due to the increase in viscosity. A test that can directly be connected to the flow of polymer melt in process is shear rate or shear stress sweeping viscometry test, as shown in Figure 8. Both PPS and the nanocomposites show steady shear viscosity with strong shear thinning behavior during the experimental shear rate range.

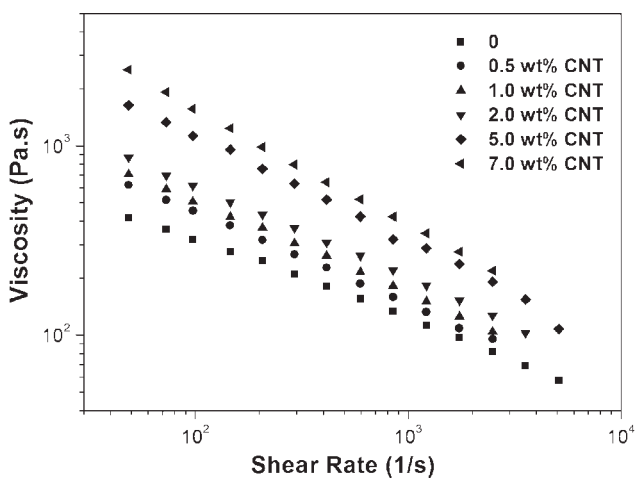


**Figure 8** Rheological properties of the PPS nanocomposites.

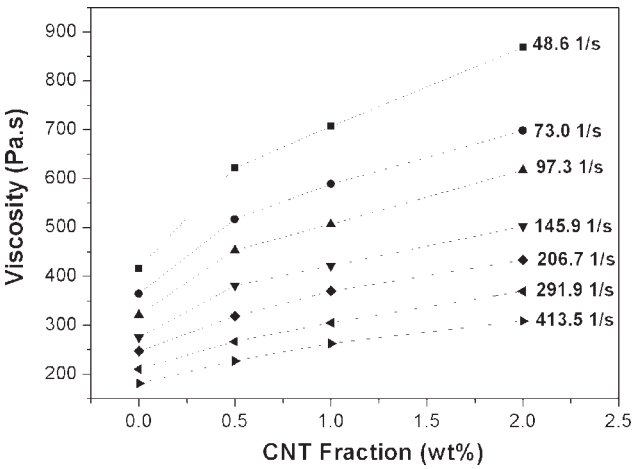


**Figure 9** Viscosity of the PPS nanocomposites versus CNT fraction at different shear rates.

This is a typical property for polymers in which the molecular chains orient themselves in the direction of the flow. Significant shear thinning property was also been observed in other kinds of nanocomposites, such as clay-reinforced polymer hybrid materials.[25,26] The viscosity of the PPS composites also increases with CNT loading, especially at lower shear rates. For example, at a shear rate of 48.6 $s^{-1}$, the viscosity for neat PPS is 416.6 Pa s, whereas the viscosity for the nanocomposite with 7 wt % of CNT loading is 2525.3 Pa s. The latter is about six times higher than the former. As a comparison, at the higher shear rate of 2493.1 $s^{-1}$, the viscosity difference for the two materials is only about two times.

Figure 9 shows the viscosity of the PPS nanocomposites as a function of CNT fraction at different shear rates. Inflexion points at 0.5 wt % of CNT can be seen in the curves, especially at low shear rates from 48.9 to 145.9 $s^{-1}$. Before this point, the viscosity shows rapid increase with CNT fraction, but after this point, the influence of the CNTs on the viscosity is not so strong. The existence of the inflexion point indicates that there is a percolation in terms of the viscosity of the nanocomposites, and this percolation threshold lies at 0–0.5 wt % of the CNTs. Morphology of the CNT networks interpenetrating into the PPS molecular chains might have an obvious change before and after the percolation threshold.

Both electrical and rheological properties of the PPS nanocomposites show sudden change with the CNT fraction, suggesting that both of them are sensitive to the interconnectivity of the CNTs in the PPS matrix to set up network and to impede polymer mobility. The sudden change is in the range of 0–0.5 wt % of CNT for viscosity and 1–2 wt % of CNT for electrical conductivity. This difference is mainly attributed to the different nanotube–nanotube distance required for the electrical conductivity and

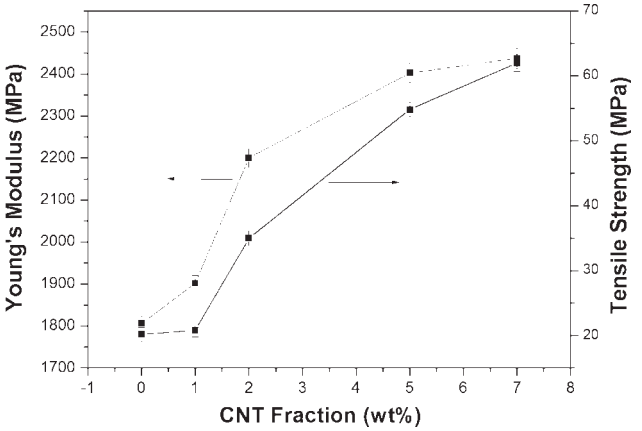


**Figure 10** Mechanical properties of the PPS nanocomposites as a function of carbon nanotube fraction.

polymer mobility.[27,28] For electrical conductance of the nanocomposites, it is assumed that the carbon nanotubes reach the percolation threshold in polymeric matrix when they have physical contact with each other or they are close enough, usually less than 5 nm, to allow electron hopping/tunneling processes. However, for the viscosity of the nanocomposites, when the distance between two nanotubes is smaller than the radius of gyration of a polymer chain in molten state, which is generally about dozens of nanometers, the carbon nanotubes can be linked by random coils of polymer chains and impede the motion of polymer chains. Thus, the viscosity of the composites will be affected by the existence of carbon nanotubes at lower loading. Moreover, the carbon nanotubes with defects contribute little to the electrical property of the materials. Therefore, a denser or broader carbon nanotube's path is required to achieve the electrical percolation threshold.

The mechanical properties of materials are always very important for their applications. Figure 10 shows the mechanical properties of the CNT reinforced PPS nanocomposites. It can be seen that both Young's modulus and tensile strength increase significantly with the increasing carbon nanotube loading. Comparing the mechanical properties of 5 wt % CNT-reinforced composite with neat PPS, the modulus increases by about 33% and tensile strength increases by about 172%, respectively. The improvements in the mechanical properties also verify the uniform dispersion of CNTs in the PPS matrix.

Figure 11 shows FESEM micrographs of fracture surfaces of the neat PPS resin and the nanocomposite containing 5 wt % of CNT. It can be seen clearly that carbon nanotubes disperse uniformly in the PPS matrix. Comparing the two fracture surfaces, the failure surface of the nanocomposite is much coarser and the nanotubes are seen clearly to be pulled out,

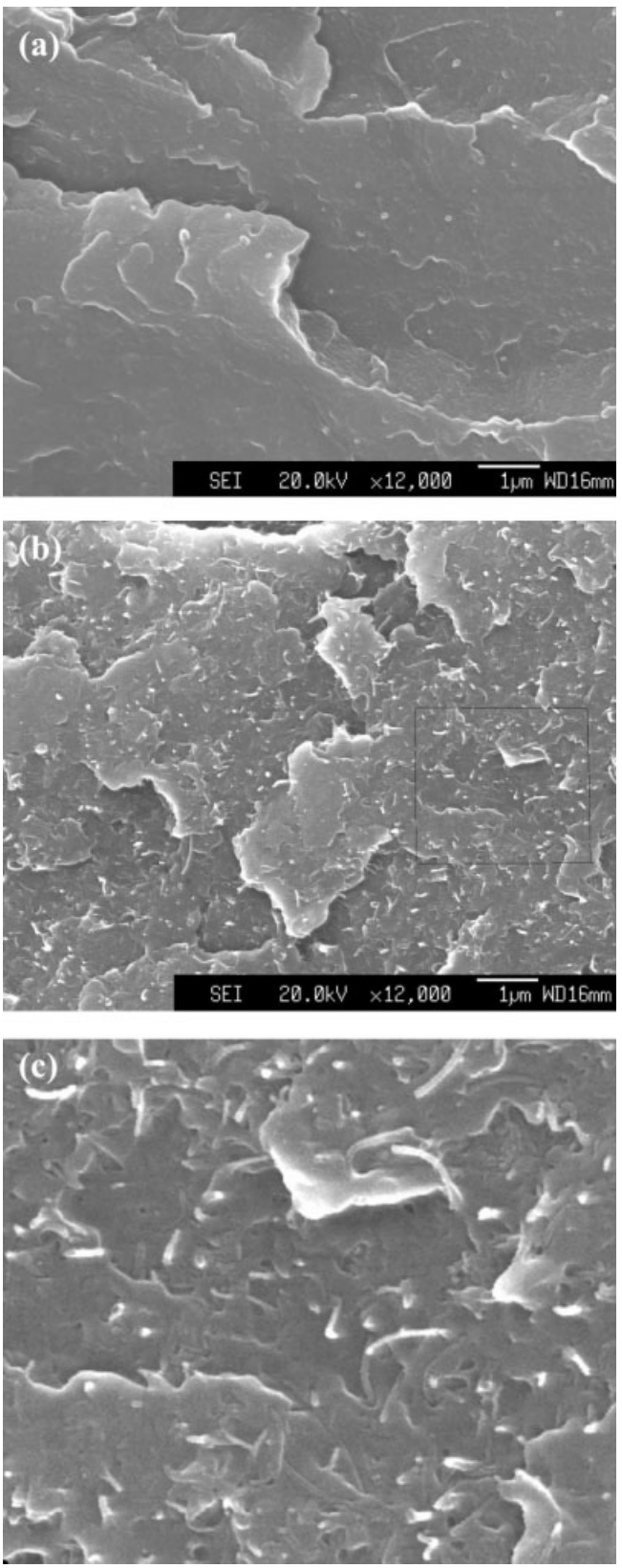


**Figure 11** FESEM micrographs of the fracture surfaces of (a) neat PPS, (b) PPS with 5 wt % of CNTs, and (c) enlarged (b).

indicating a certain degree of load transfer from the resin to the carbon nanotubes, so higher tensile strength is obtained for the nanocomposite.

## CONCLUSIONS

Carbon nanotube-reinforced PPS nanocomposites with significant improved electrical, thermal, and mechanical properties have been successfully fabricated through melt compounding. The electrical resistivity of the derived nanocomposites is about $1.12 \times 10^5$ Ω cm at CNT concentration as low as 2 wt %. The resultant electrical resistivity is also temperature independent in the experimental range. The incorporation of carbon nanotubes into PPS shows significant improvement in thermal stability of the nanocomposites but a decrease in their crystallization rate. For the rheological behavior, both neat polymer and its nanocomposites show shear thinning behavior. The rheological threshold observed is lower as compared with the electrical threshold. The addition of carbon nanotubes into the polymer also has great impact on the mechanical properties of the nanocomposites. Both modulus and tensile strength of the nanocomposites increase significantly with increasing carbon nanotube fraction. The morphology analysis on fracture surfaces indicates that the enhancement of carbon nanotubes on the mechanical properties is due to a certain degree of load transfer from resin to the CNT fillers.

The experimental results of the nanocomposites present a very positive prospect to industry applications.

## References


1. Rupprecht, L. Conductive Polymers and Plastics in Industrial Applications; Plastics Design Library: Norwich, NY, 1999.
2. Akbar, E. A.; Massoumi, B. Curr Trends Polym Sci 2004, 9, 81.
3. Ebbesen, T. W.; Lezec, H. J.; Hiura, H.; Bennett, J. W.; Ghaemi, H. F.; Thio, T. Nature 1996, 382, 54.
4. Treacy, M.; Ebbesen, T. W.; Gibson, J. M. Nature 1996, 381, 678.
5. Cochet, M.; Maser, W. K.; Benito, A. M.; Callejas, A.; Martínez, M. T. Chem Commun 2001, 16, 1450.
6. Zengin, H.; Zhou, W.; Jin, J.; Czerw, R.; Smith, D. W.; Echegoyen, L, Jr.; Carroll, D. L.; Foulger, S. H.; Ballato, J. Adv Mater 2002, 14, 1480.
7. Saeed, K.; Park, S.-Y. J Appl Polym Sci 2007, 106, 3729.
8. Safadi, B.; Andrews, R.; Grulke, E. A. J Appl Polym Sci 2001, 84, 2660.
9. Cadek, M.; Coleman, J. N.; Barron, V.; Hedicke, K.; Blau, W. J. J. Proc SPIE 2002, 4876, 676.
10. Shaffer, M. S. P.; Windle, A. H. Adv Mater 1999, 11, 937.
11. Clayton, L. M.; Sikder, A. K.; Kumar, A.; Cinke, M.; Meyyappan, M.; Gerasimov, T. G.; Harmon, J. P. Adv Funct Mater 2005, 15, 101.
12. Andrews, R.; Jacques, D.; Minot, M.; Rantell, T. Macromol Mater Eng 2002, 287, 395.
13. Lozano, K.; Barrera, E. V. J Appl Polym Sci 2001, 79, 125.
14. Pötschke, P.; Fornes, T. D.; Paul, D. R. Polymer 2002, 43, 3247.
15. Biederman, H. Polymer Physics; Springer-Verlag: Berlin, 1990.
16. Available at: http://www.dic.co.jp/eng/products/pps/polymer.html.
17. Scobbo, J. J.; Hwang, C. R. Polym Eng Sci 1994, 34, 23.
18. McKetta, J. J.; Cunningham, W. A. In Polymers, Polyamides, Aromatic to Polymers, Polyvinylchloride; Encyclopedia of Chemical Processing and Design; Marcel Dekker: New York, 1992, p 94–125.
19. Lee, T. H.; Boey, F. Y. C.; Khor, K. A. Compos Sci Technol 1995, 53, 259.
20. Li, S.; Qin, Y.; Shi, J.; Guo, Z.; Li, Y.; Zhu, D. Chem Mater 2005, 17, 130.
21. Ramasubramaniam, R.; Chen, J.; Liu, H. Appl Phys Lett 2003, 83, 2928.
22. Mclachlan, D. S.; Chiteme, C.; Park, C.; Wise, K. E.; Lowther, S. E.; Lillehei, P. T.; Siochi, E. J.; Harrison, J. S. J. J Polym Sci Part B: Polym Phys 2005, 43, 3273.
23. Barraza, H. J.; Pompeo, F.; O'Rear, E. A.; Resasco, D. E. Nanoletters 2002, 2, 797.
24. Hoffman, J. D.; Davis, G. T.; Lauritzen, J. I. In Treatise on Solid State Chemistry; Plenum Press: New York, 1976; Vol. 3, p 7.
25. Yu, S.; Liu, S.; Zhao, J.; Xie, H.; Yong, M. S. Polym Polym Compos 2006, 14, 271.
26. Krishnamoorti, R.; Vaia, R. A.; Giannelis, E. P. Chem Mater 1996, 8, 1728.
27. Potschke, P.; Abdel-Goad, M.; Alig, I.; Dudkin, S. Polymer 2004, 45, 8863.
28. Du, F.; Scogna, R. C.; Zhou, W.; Brand, S.; Fischer, J. E.; Winey, K. I. Macromolecules 2004, 37, 9048.